Copy 1.

RM SA52C10



NACA

# RESEARCH MEMORANDUM



for the



Ordnance Corps, Department of the Army

## INVESTIGATION IN THE AMES SUPERSONIC FREE-FLIGHT WIND TUNNEL OF THE STATIC LONGITUDINAL STABILITY OF THE HERMES A-3B MISSILE AT A MACH NUMBER OF 5.0

By Thomas N. Canning and Billy Pat Denardo

Ames Aeronautical Laboratory
Moffett Field, Calif.



## NATIONAL ADVISORY COMMITTEE FOR AERONAUTICS

WASHINGTON

Mar. 10, 1952

 

NATIONAL ADVISORY COMMITTEE FOR AERONAUTICS

RESEARCH MEMORANDUM

for the

Ordnance Corps, Department of the Army

# INVESTIGATION IN THE AMES SUPERSONIC FREE-FLIGHT WIND TUNNEL OF THE STATIC LONGITUDINAL STABILITY OF THE HERMES A-3B MISSILE AT A MACH NUMBER OF 5.0

By Thomas N. Canning and Billy Pat Denardo

## SUMMARY

Models of the Hermes A-3B missile were tested in the Ames supersonic free-flight wind tunnel to determine the static-longitudinal-stability characteristics at a Mach number of 5.0 and a Reynolds number based on body length of 10 million. The results indicated that the model center of pressure was 45.3 percent of the body length aft of the nose and the lift-curve slope based on body frontal area was 0.064 per degree. Estimates indicated that the effect on these characteristics of aeroelastic twisting of the model fins was small but important if a precise location of center of pressure is required. A comparison of the test results with predictions based on available theory showed that the theory was useful only for rough estimates.

The drag coefficient at zero lift, based on body frontal area, was found to be 0.155.

## INTRODUCTION

At the request of the Ordnance Corps, Department of the Army, tests were conducted in the Ames supersonic free-flight wind tunnel to determine the static-longitudinal-stability characteristics of the Hermes A-3B missile at a Mach number of 5.0 and a Reynolds number of 10 million. These tests were intended to supplement those being performed in other facilities at somewhat different conditions; some at lower Mach numbers and others at lower Reynolds numbers. The principal objective of this test was to determine experimentally the center-of-pressure location near zero angle of attack. The test Reynolds number was dictated by the need

for data at this Mach number with attached, turbulent boundary-layer flow over the body boattail. Shadowgraph pictures showed that this requirement was met. The experiments also made possible the determination of lift-curve slope and drag coefficient at zero lift.

The experimentally determined values of lift-curve slope and center of pressure were compared with values predicted using existing theories which are based in part on the assumption of small perturbations. This assumption was violated seriously in the present case because the model was quite blunt and the Mach number was high. The comparison is presented to gain some insight into the usefulness of such theories under such conditions.

Since the stabilizing fins of this configuration are very thin and the dynamic pressure of the tests was about 150 pounds per square inch, an estimate of the influence of aeroelasticity on the longitudinal characteristics of the test configuration is included.

## SYMBOLS

| | |
|---|---|
| $c$ | tail chord, feet |
| $C_D$ | coefficient of drag $\left(\frac{\text{drag force}}{Sq_o}\right)$ |
| $C_{D_{min}}$ | coefficient of drag at zero lift |
| $C_L$ | coefficient of lift $\left(\frac{\text{lift force}}{Sq_o}\right)$ |
| $C_{L_\alpha}$ | lift-curve slope $\left(\frac{dC_L}{d\alpha}\right)$, per degree |
| $l$ | body length, feet |
| $q_o$ | free-stream dynamic pressure, pounds per square foot |
| $S$ | maximum cross-sectional area of model body, square feet |
| $t$ | tail thickness, feet |
| $X$ | axial distance along model, feet |

$X_{c.p.}$ center-of-pressure position aft of nose, feet

$\alpha$ angle of attack, degrees

## APPARATUS, TECHNIQUES, AND MODELS

### Facility

The tests were conducted in the Ames supersonic free-flight wind tunnel. This facility is a short ballistic range inside a variable pressure, supersonic, blowdown wind tunnel. In this tunnel, models are fired upstream through the 15-foot test section at high velocity from a gun located in the diffuser while the tunnel is operating at a Mach number of 2.0. The aerodynamic data are obtained from a history of the model motion, as recorded by seven shadowgraph stations and a chronograph. Details of tunnel operation are given in reference 1.

### Techniques

In order to obtain the center-of-pressure location, both the lift-curve and pitching-moment-curve slopes were determined. The former was found by comparing the time history of the model angle of attack with the curvature of the flight path due to lift. The pitching-moment-curve slope was obtained from the frequency of oscillation in pitch, assuming that the moment curve was linear within the experimental range of angle of attack, that the damping in pitch was proportional to the pitching rate, and that there was no aerodynamic interaction between pitch and yaw. Details of the technique of data analysis are given in reference 1. Since the models were free to roll, the possibility that the rolling might alter the model stability was investigated. In no case was the model rolling frequency greater than one fourth the pitching frequency so that no important effects were indicated (reference 2). It is believed that the rolling during the tests obscured any effects of roll position on lift-curve slope and center of pressure and that the results represent average values over a range of roll positions.

The time history of model position was also used to determine deceleration and hence drag. The calculations were based on the assumption that $C_D$ is constant. Since, in these tests, angles of attack of about $6^{\circ}$ were experienced, the varying drag due to lift was important. The effect of this varying drag, although not treated exactly, was accounted for approximately by subtracting from the indicated average value of $C_D$ an approximate value of drag due to lift given by the mean value during test of the expression $C_{L_\alpha} \alpha \tan \alpha$.

### Models

The models used in this investigation were 0.0073-scale models of the Hermes A-3B missile with the smallest of the three tail fins proposed. (See fig. 1(a)). The fins of all the models were made of 75 S-T aluminum and were continuous through the body. The bodies were made of various metals to give the desired masses and centers of gravity. Shadowgraphs of a typical model in flight are presented in figure 2. The required pitching oscillations were initiated by firing the model from the gun in a plastic carrier called a sabot, which held the model at $5^{\circ}$ angle of attack until shortly after the sabot-model assembly left the gun.

## THEORETICAL CALCULATIONS

### Theoretical Load Distributions

In an attempt to gain some insight as to the usefulness of available theories for estimating longitudinal characteristics of fin-body combinations at high Mach numbers, values of lift-curve slope and center of pressure of this model were predicted using several theoretical approaches which differed only in the method of estimating the characteristics of the body. The linear theory (reference 3) could not be applied directly to this body because the nose-cone angle is greater than the Mach angle at Mach number 5.0. Two of the three methods described involved arbitrary assumptions to overcome this difficulty. The methods used are described below, and the resulting lift distributions are shown in figure 3:

I. The lift on the relatively blunt nose cone was estimated using reference 4. The lift distribution on the remainder of the body was calculated using reference 3, assuming that the nose is extended to the apex of the second conical section as shown in figure 1(b).

II. The lift distribution on the forward portion of the extended-nose configuration of method I was calculated using reference 4, and the portion of the lift on the extension was arbitrarily distributed along the real configuration in such a manner that there were no discontinuities in the lift distribution at the nose-cone juncture as shown in figure 3. The amount of lift involved in the redistribution is small, so that any other reasonable distribution would yield similar results. The lift on the remainder of the body was calculated using reference 3.

III. The lift distribution for the entire body was calculated using slender-body theory (reference 5).

The lift and moment contributions of the tail fins and fin-body interference were estimated on the basis of references 6 and 7, using the tail configuration shown in figure 1(c). Since most of the fin area was ahead of the Mach wave from the leading edge of the root chord, the lifting pressures were calculated using shock-expansion theory in this area at the Mach number normal to the leading edge. No account was taken of boundary-layer interference on lift of the wing or body.

The rather diverse results of these calculations are shown in the following table:

| Method | Body | | Fins and interference | | Complete model | |
|---|---|---|---|---|---|---|
| | $C_{L_\alpha}$ | $\frac{x_{c.p.}}{l}$ | $C_{L_\alpha}$ | $\frac{x_{c.p.}}{l}$ | $C_{L_\alpha}$ | $\frac{x_{c.p.}}{l}$ |
| I | 0.0395 | 0.194 | 0.0216 | 0.957 | 0.0611 | 0.465 |
| II | .0519 | .209 | .0216 | .957 | .0735 | .430 |
| III | .0161 | -.420 | .0216 | .957 | .0377 | .370 |

Method III gives results which differ greatly from the other results. This difference lies in the prediction of negative lift over all the body aft of the maximum thickness point, while positive lift is predicted over most of this region by the method of reference 3 used in the other two calculations. At lower Mach numbers the methods would give more consistent answers.

## Estimation of Aeroelastic Effects

The twist of the tail fins under aerodynamic loads was estimated roughly in order to assess the difference between the results obtained with the actual test models and what would have been measured had the models been absolutely rigid. In the calculations the load distribution predicted by linearized theory for a rigid wing was used. The actual model and test conditions fixed the fin material and dynamic pressure. In order to simplify the calculations the solid, double-wedge profile was replaced with a solid elliptical section of equal area and polar moment of inertia, as suggested in reference 8.

These calculations indicated a loss of about 10 percent of the rigid-wing lift. If the theoretical division of lift between tail and body, as given by method I above, had been used, this loss of tail lift would result in approximately a 3 percent loss in $C_{L_\alpha}$ and about

a 2 percent forward shift in center of pressure. Bending, as well as twisting, results from the loads and causes additional loss of lift. Calculations have shown that this effect is somewhat smaller than the twisting effect. The two deformations are interconnected in a very complex manner, however, so the only deformation considered in these calculations was twist. It is believed that the aeroelastic effect is underestimated.

## RESULTS AND DISCUSSION

The mean experimental value of lift-curve slope from three tests was 0.064 with ±11-percent scatter about this value. The center of pressure was 45.3 ± 0.7 percent of the body length aft of the nose. If the estimated effects of aeroelasticity are applied as corrections to the experimental results the rigid-model values would be $C_{L_\alpha} = 0.066$ and $X_{c.p.}/l = 0.470$. The theoretical results obtained by methods I and II are of the right magnitude for both $C_{L_\alpha}$ and $X_{c.p.}$ Method I, which gives $C_{L_\alpha} = 0.0611$ and $X_{c.p.}/l = 0.465$, is sufficiently accurate to be of value. Because of the arbitrary method of treating the nose cone, however, it is probable that the agreement is fortuitous. The results of method III, using slender-body theory, were inaccurate by comparison. In addition to giving rough answers for the absolute values of $C_{L_\alpha}$ and $X_{c.p.}/l$, methods I and II are believed to be excellent bases for calculating the effects of small design variations such as changes in fin size.

The drag coefficient at zero lift of this model was 0.155 based on the body frontal area. This result is based on only two tests and the scatter between the two determinations was ±6 percent of the mean value.

## CONCLUDING REMARKS

Tests of the Hermes A-3B missile at a Mach number of 5.0 and a Reynolds number based on body length of 10 million indicate the following mean results:

| | $C_{L_\alpha}$ | $\frac{X_{c.p.}}{l}$ | $C_{D_{min}}$ |
|---|---|---|---|
| Uncorrected for aeroelasticity | 0.064 | 0.453 | 0.155 |
| Corrected for aeroelasticity | .066 | .470 | .155 |

The theoretical methods used in this report appear useful for rough estimates of the lift and center of pressure of this missile at a Mach number of 5, and are believed to be useful for predicting changes in these quantities resulting from small design changes.

Ames Aeronautical Laboratory
National Advisory Committee for Aeronautics
Moffett Field, Calif.

REFERENCES

1. Seiff, Alvin, James, Carlton S., Canning, Thomas N., and Boissevain, Alfred G.: The Ames Supersonic Free-Flight Wind Tunnel. NACA RM A52A24, 1952.

2. Phillips, William H.: Effect of Steady Rolling on Longitudinal and Directional Stability. NACA TN 1627, 1948.

3. Tsien, Hsue-Shen: Supersonic Flow Over an Inclined Body of Revolution. Jour. of Aero. Sci., Oct. 1938, pp. 480-483.

4. Mass. Inst. of Tech., Dept. of Elect. Engr., Center of Analysis. Tables of Supersonic Flow Around Yawing Cones, by the Staff of the Computing Section, under the direction of Zdenek Kopal. Tech. Rept. No. 3., Cambridge, 1947.

5. Munk, Max M.: The Aerodynamic Forces on Airship Hulls. NACA Rep. 184, 1924.

6. Nielsen, Jack N., and Kaattari, George E.: Method for Estimating Lift Interference of Wing-Body Combinations at Supersonic Speeds. NACA RM A51J04, 1951.

7. Nielsen, Jack N., Kaattari, George E., and Pitts, William C.: Method for Estimating Pitching-Moment Interference of Wing-Body Combinations at Supersonic Speeds. NACA RM A52B06, 1952.

8. Timoshenko, S.: Strength of Materials - Part II, Advanced Theory and Problems. 2d ed. D. Van Nostrand Company, Inc., N. Y., 1940-41.

FIGURE LEGENDS

Figure 1.- Experimental and theoretical models of Hermes A-3B.
(a) Experimental body. (b) Extended nose. (c) Tail.

Figure 2.- Model in flight at $M = 5.0$, $R = 10$ million.
(a) $\alpha \approx 0^\circ$ (b) $\alpha \approx 6^\circ$

Figure 3.- Theoretical load distributions on the body.

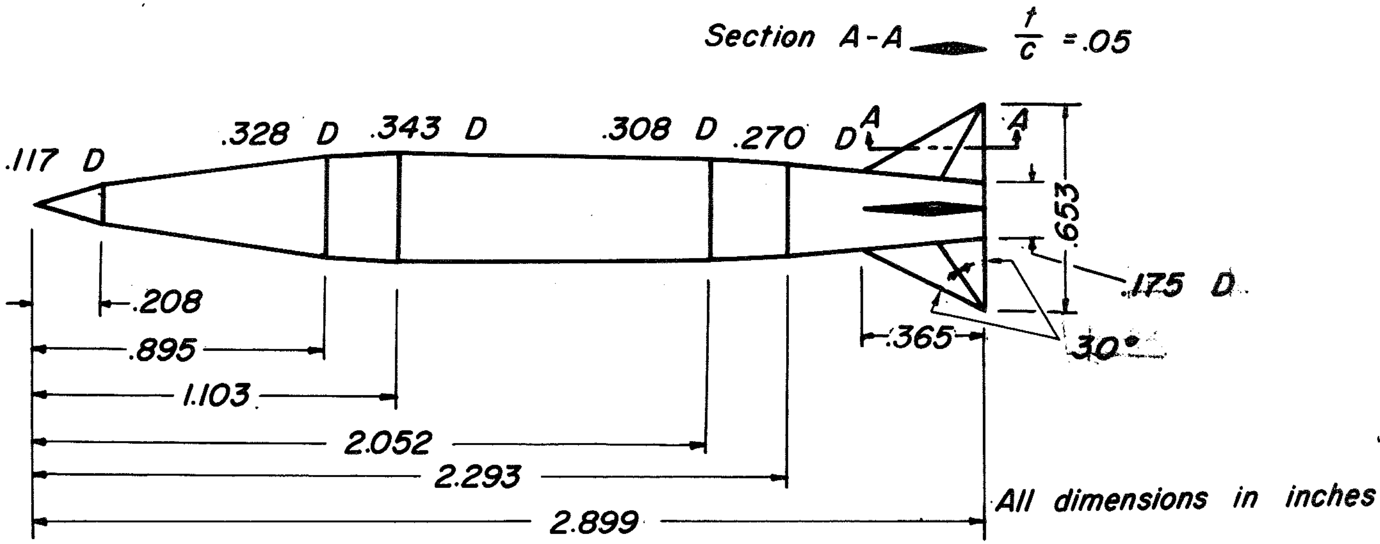


(a) Experimental body.

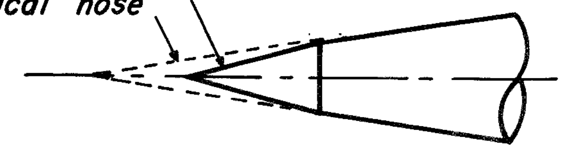


(b) Extended nose.

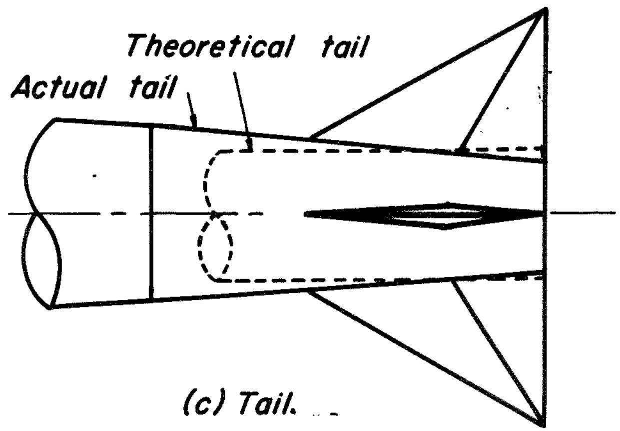


(c) Tail.

Figure 1.- Experimental and theoretical models of Hermes A-3B.

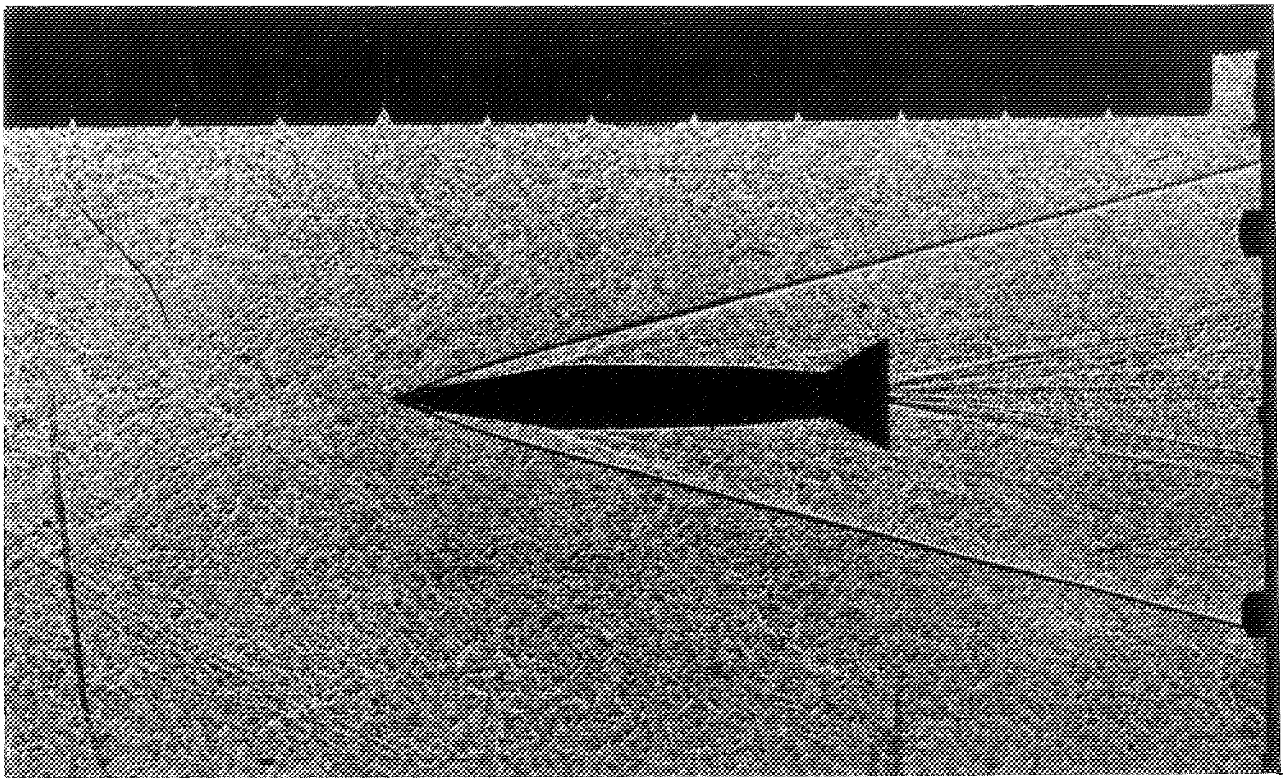

(a) $\alpha \approx 0°$

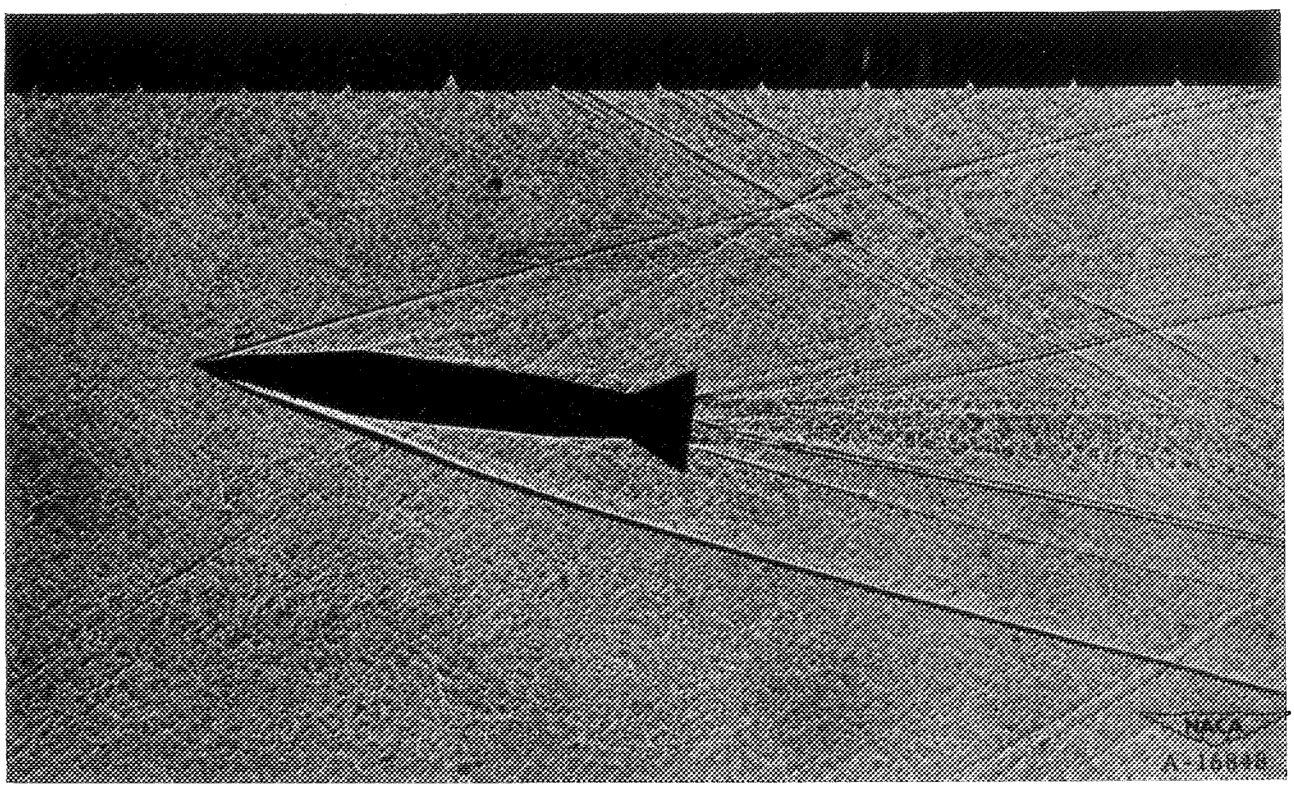


(b) $\alpha \approx 6°$

Figure 2.- Model in flight at M = 5.0, R = 10 million.

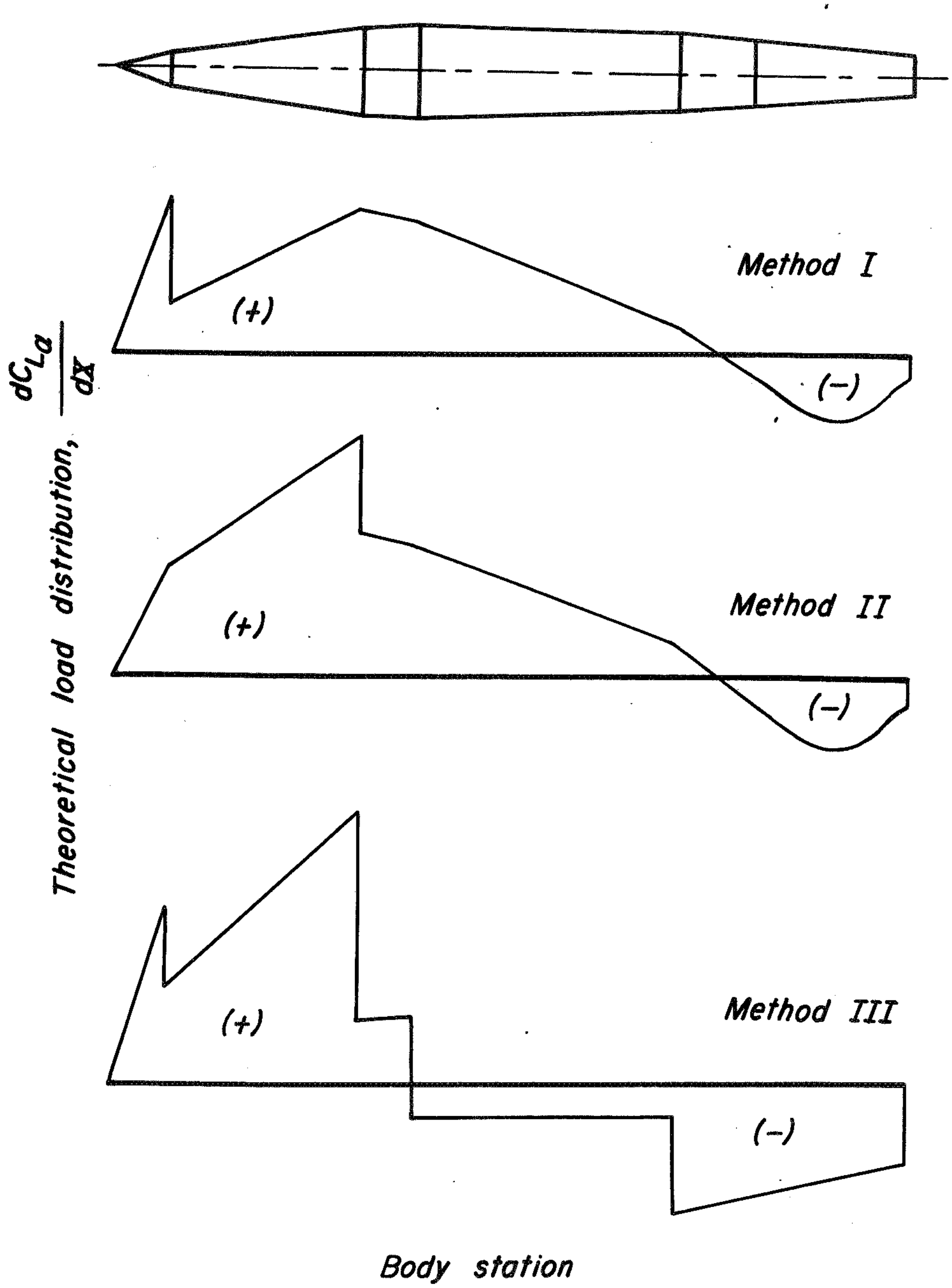


Figure 3.- Theoretical load distributions on the body.